

Supporting Information of Water Facilitates Oxygen Migration on Gold Surfaces

Fang Xu,¹ Ioanna Fampiou,¹ Christopher R. O'Connor,¹ Stavros Karakalos,^{1,†} Fanny Hiebel,¹ Efthimios Kaxiras,^{2,3} Robert J. Madix,³ Cynthia M. Friend^{1,3,*}

¹Department of Chemistry and Chemical Biology, Harvard University, Cambridge, MA 02138, USA

²Department of Physics, Harvard University, Cambridge, Massachusetts 02138, USA

³John A. Paulson School of Engineering and Applied Sciences, Harvard University, Cambridge, Massachusetts 02138, USA

1. Quantitative Analysis Methods

1.1 Temperature-programmed Reaction Spectroscopy

In the quantitative analysis, the consideration of the molecular fragmentation pattern and ionization cross-section, and the mass spectrometer transmission and detection coefficients is necessary. It has been shown elsewhere¹ that the number density of molecule *i* in the ionizer, n_i , is given as follows:

$$n_i = \frac{\sigma_i^{-1} \cdot s_{ik}}{T_{ik} \cdot \delta_{ik}} \cdot \left(1 + \sum_j \frac{s_{ij}}{s_{ik}} \cdot \frac{T_{ik} \cdot \delta_{ik}}{T_{ij} \cdot \delta_{ij}} \right) \quad (1)$$

where

σ_i is the total ionization cross-section of molecule *i*,

s_{ik} is the measured signal current for the *k*th fragment of molecule *i*,

s_{ij}/s_{ik} is the ratio of signals of the *j*th and *k*th fragments of molecule *i* determined from separate calibrations of the neat parent molecule *i*,

T_{ik} is the transmission coefficient of a fragment with *m/z*, *k*, of molecule *i*,

T_{ij} is the transmission coefficient of a fragment with *m/z*, *j*, of molecule *i*,

δ_{ik} is the detection coefficient of a fragment with *m/z*, *k*, of molecule *i*,

δ_{ij} is the detection coefficient of a fragment with *m/z*, *j*, of molecule *i*.

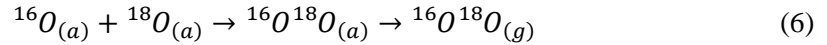
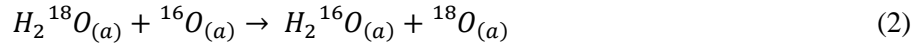
In the equation above, the constants σ_i , T_{ik} , T_{ij} , δ_{ik} and δ_{ij} are taken from published values (Table S1). s_{ij}/s_{ik} is determined for molecule *i* by condensing a neat sample of molecule *i* on clean Au(110) and the fragmentation pattern was recorded by TPRS.

Table S1. Mass Spectrometry quantitative analysis constants

m/z	Transmission Coefficient ^a	Detection Coefficient ^b	Molecule	Ionization Cross-section ^c
0-20	1	1.5	H ₂ O	2.275
21-30	1	1	O ₂	2.441
31-40	1	0.9		

^a Adapted from Hiden manual^b Adapted from UTI manual^c Values calculated at an incident electron voltage of 70 eV from the NIST database

The extent of oxygen exchange can be calculated from the stoichiometric relations of the following reactions for H₂¹⁸O and ¹⁶O.



The amount of replaced ¹⁶O can be determined by two methods based on desorption peak areas: by the amount of H₂¹⁶O formed (equation 8), and by the amount of ¹⁸O from all of oxygen molecules (equation 9).

$${}^{16}O_{\text{extent of replacement}} = \frac{H_2^{16}O_{(g)}}{H_2^{16}O_{(g)} + H_2^{18}O_{(g)}} \quad (8)$$

$${}^{16}O_{\text{extent of replacement}} = \frac{{}^{16}O^{18}O_{(g)} + 2 \cdot {}^{18}O_{2(g)}}{2 \cdot {}^{16}O_{2(g)} + {}^{16}O^{18}O_{(g)} + 2 \cdot {}^{18}O_{2(g)}} \quad (9)$$

Experiments performed below the desorption temperature of water confirmed that the extent of ¹⁶O replacement agrees well for both methods.

1.2 Scanning Tunneling Microscopy

Commercialized software Scanning Probe Image Processor (SPIPTM) version 6.0.2 (Image Metrology) was used to analyze the time evolution of STM images of O/Au(110) under H₂O. ($\theta_0=0.04$ ML, $P_{H_2O}=3 \times 10^{-10}$ Torr). The difference of the same area in the recording sequence was obtained by subtracting the previous image from the next one. Each terrace was analyzed separately to avoid height interference between different terraces (Fig. S1A). Since oxygen is imaged as dark in STM, the disappeared oxygen is bright feature, and appeared oxygen is dark feature. The disappeared and appeared

oxygen chains can be explicitly shown along $\langle 1\bar{1}0 \rangle$ direction (Fig. S1B), thereafter, their length can be checked manually and then calculated using the software. Under the assumption that only zig-zag single row oxygen chains are formed at 0.04 ML of oxygen coverage,² the number of migrated oxygen atoms is calculated by divide the total length along $\langle 1\bar{1}0 \rangle$ direction over 0.288 nm, the short edge of Au(110) unit cell.

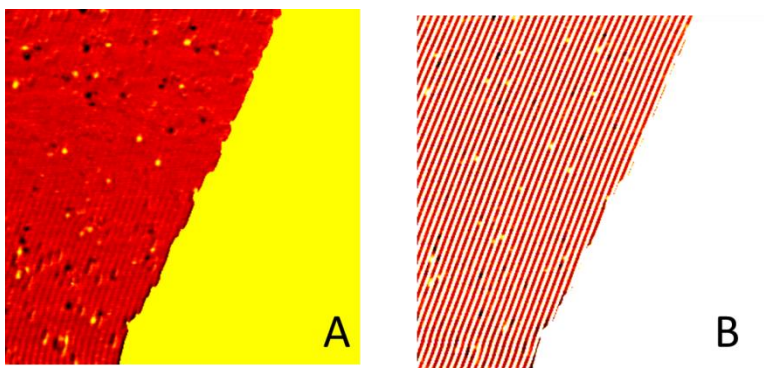


Figure S1. Quantitative analysis of surface evolution based on a sequence of STM images. (A) The difference between neighboring images of one terrace, the disappeared and appeared oxygen corresponds to bright and dark features respectively. (B) the feature highlighted along $\langle 1\bar{1}0 \rangle$ direction.

2. Supporting Results

2.1 Water desorption temperature on Au(110) and O/Au(110)

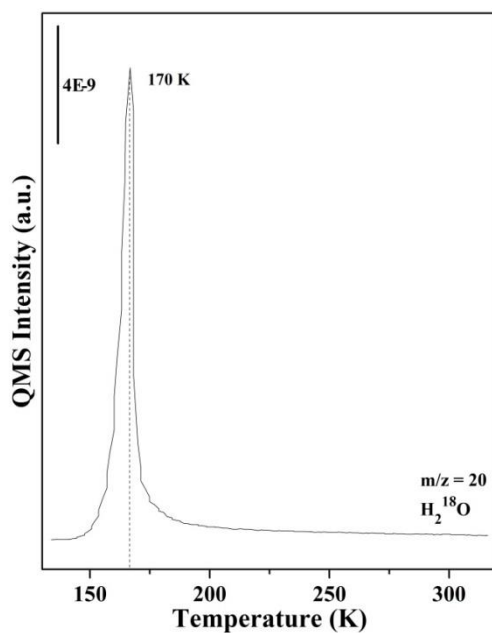


Figure S2. TPRS of H₂¹⁸O desorption from clean Au(110) surface. m/z = 20.

1.0×10^{-11} Torr of H_2^{18}O was exposed to clean Au(110) at 120 K for 90 s. The molecularly adsorbed H_2^{18}O on clean Au(110) desorbs as a single peak at 170 K, Fig. S1. No other feature except H_2^{18}O desorption has been observed. Thus, water adsorb weakly on Au(110), and the H_2^{18}O is 100% pure.

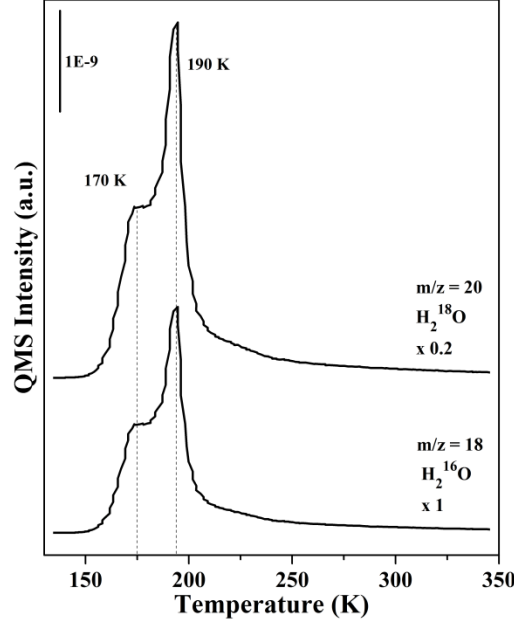


Figure S3. TPRS experiments show both isotopic combinations (H_2^{16}O and H_2^{18}O) desorb from adsorbed ^{16}O on Au(110) ($\theta = 0.04$ ML).

After 1.0×10^{-11} Torr of H_2^{18}O was exposed to 0.04 ML of $^{16}\text{O}/\text{Au}(110)$ at 130 K for 60 s, both isotopic combinations (H_2^{16}O and H_2^{18}O) were detected at 170 K and 190 K, Fig. S2, indicating the exchange of $^{16}\text{O}/\text{Au}(110)$ with H_2^{18}O . Adsorbed oxygen modifies physical and electronic structures of Au(110), creating a new site for water adsorption, which desorbs at 190 K. Using Redhead³ analysis, the activation energy is given by,

$$E_d = RT_d \left[\ln \left(\frac{\nu T_d}{\beta} \right) - \ln \left(\frac{E_d}{RT_d} \right) \right] \quad (10)$$

where E_d is the activation energy of desorption, T_d is the desorption temperature, R is the ideal gas constant. Using two peaks at 170 K and 190 K, the experimentally controlled heating rate, $\beta = 5$ K/s, and the preexponential factor (ν) for desorption is calculated based on Campbell's methods.⁴ The preexponential factor is estimated to be $4.43 \times 10^{14} \text{ s}^{-1}$, which leads to an activation energy of 48 kJ/mol (170 K peak) and 53 kJ/mol (190 K peak). Thus, the steady state concentration of water (c_w), can be calculated based on the following equations:

$$Z_w = \frac{sp}{\sqrt{2\pi mk_b T}} \quad (11)$$

$$D_w = v_o c_w e^{-\frac{E_{des}}{RT_s}} \quad (12)$$

$$c_w = \frac{sp}{v_0 e^{\frac{E_{des}}{RT_s}} \sqrt{2\pi m k_b T}} \quad (13)$$

where Z_w is the adsorption rate,⁵ D_w is desorption rate,⁶ s is the sticking coefficient, p is the H₂O vapor pressure; m is the mass of H₂O, k_b is Boltzmann's constant; T is the temperature of gas, (300 K in the experiments), E_{des} is the activation energy for desorption of water, R is the ideal gas constant, and T_s is the temperature of the substrate.

2.2 Surface structures influenced by oxygen migration

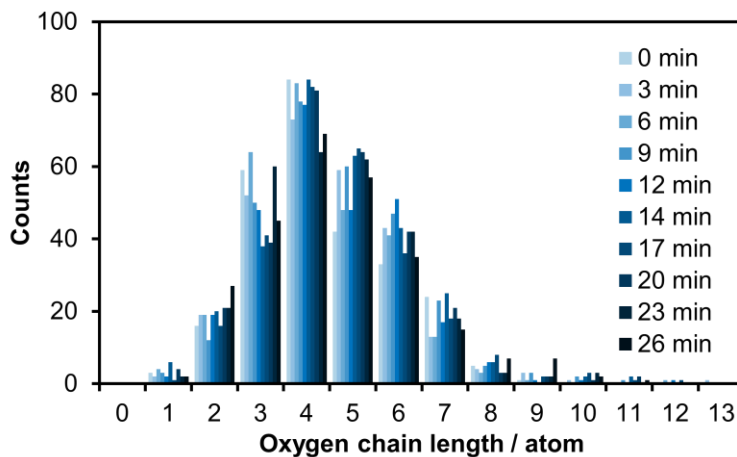


Figure S4. Histogram sequence of oxygen chain length distribution change over 26 min on 0.04 ML O/Au(110) at ~170 K under 3×10^{-10} Torr water vapor. The corresponding water exposure time is indicated in the legend. The chain length is rounded to the nearest integer.

Surface oxygen chain length distribution over water exposure time is shown in Fig. S4. The measurements are based on continuous STM images on an Au(110) area of $43 \times 43 \text{ nm}^2$, under assumption that all of the surface oxygen chains are in zig-zag structure as calculated by DFT.² When 3×10^{-10} Torr water was directly dosed to 0.04 ML O/Au(110) at ~170 K, oxygen chain length distribution doesn't significantly change over time. The major oxygen chains are composed with 3 – 7 oxygen atoms.

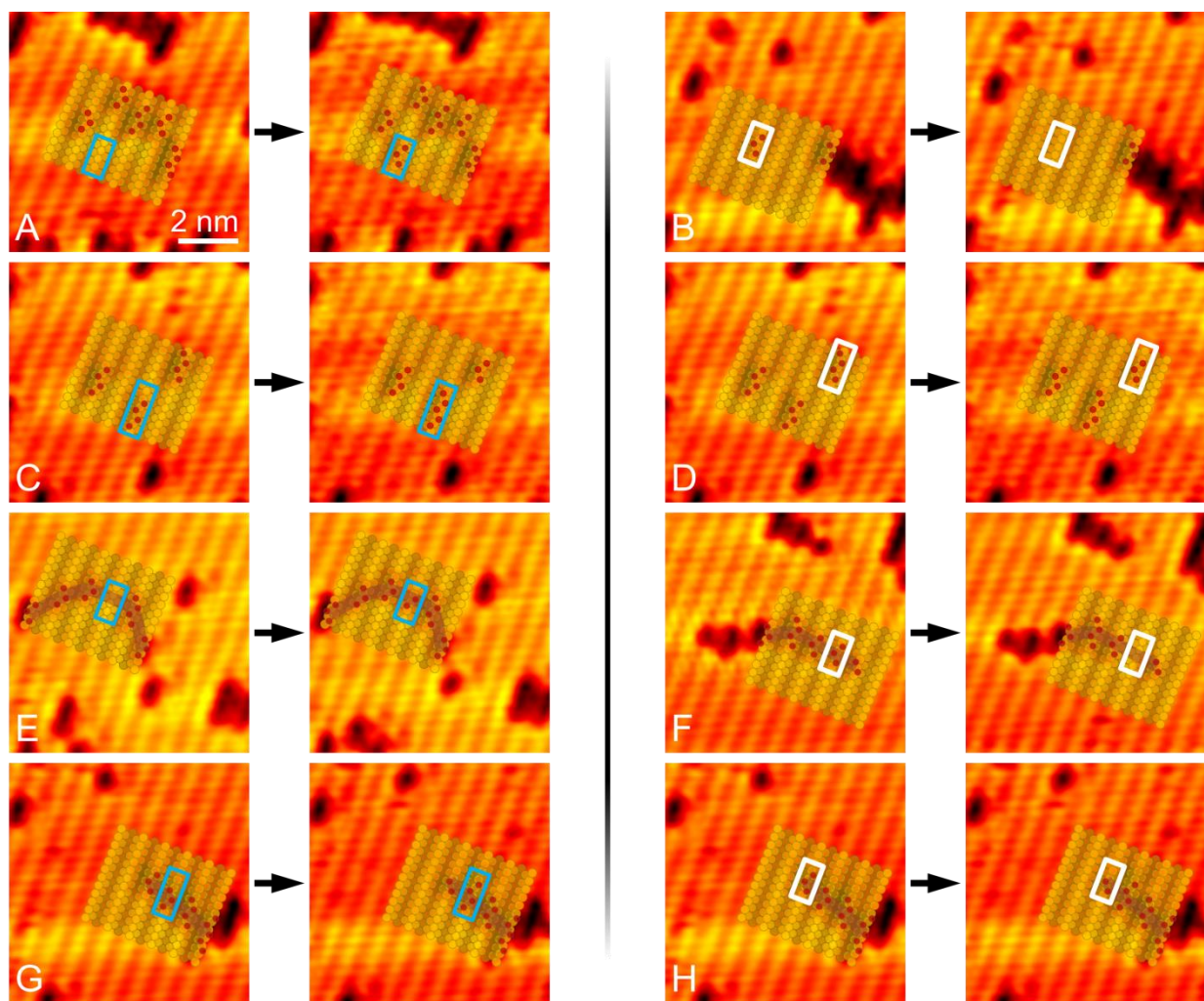


Figure S5. *In situ* STM images of a few O migration events ($\theta_0=0.04$ ML; $T_{\text{surf}}\sim 170$ K; $p(\text{H}_2\text{O})= 3\times 10^{-10}$ Torr). In each panel, the same area was imaged before and after exposure to water for 3 min. The left four panels show the addition of oxygen atoms (blue boxes); the right four panels shows the corresponding loss of oxygen atoms (white boxes). Image size: 8×8 nm²; scanning parameters: 0.1 nA; 1.4 V. Superimposed profiles are drawn to guide reading. Gold balls are Au atoms; red balls on-top are oxygen atoms. The dark bands in E, F, G and H link group oxygen chains.

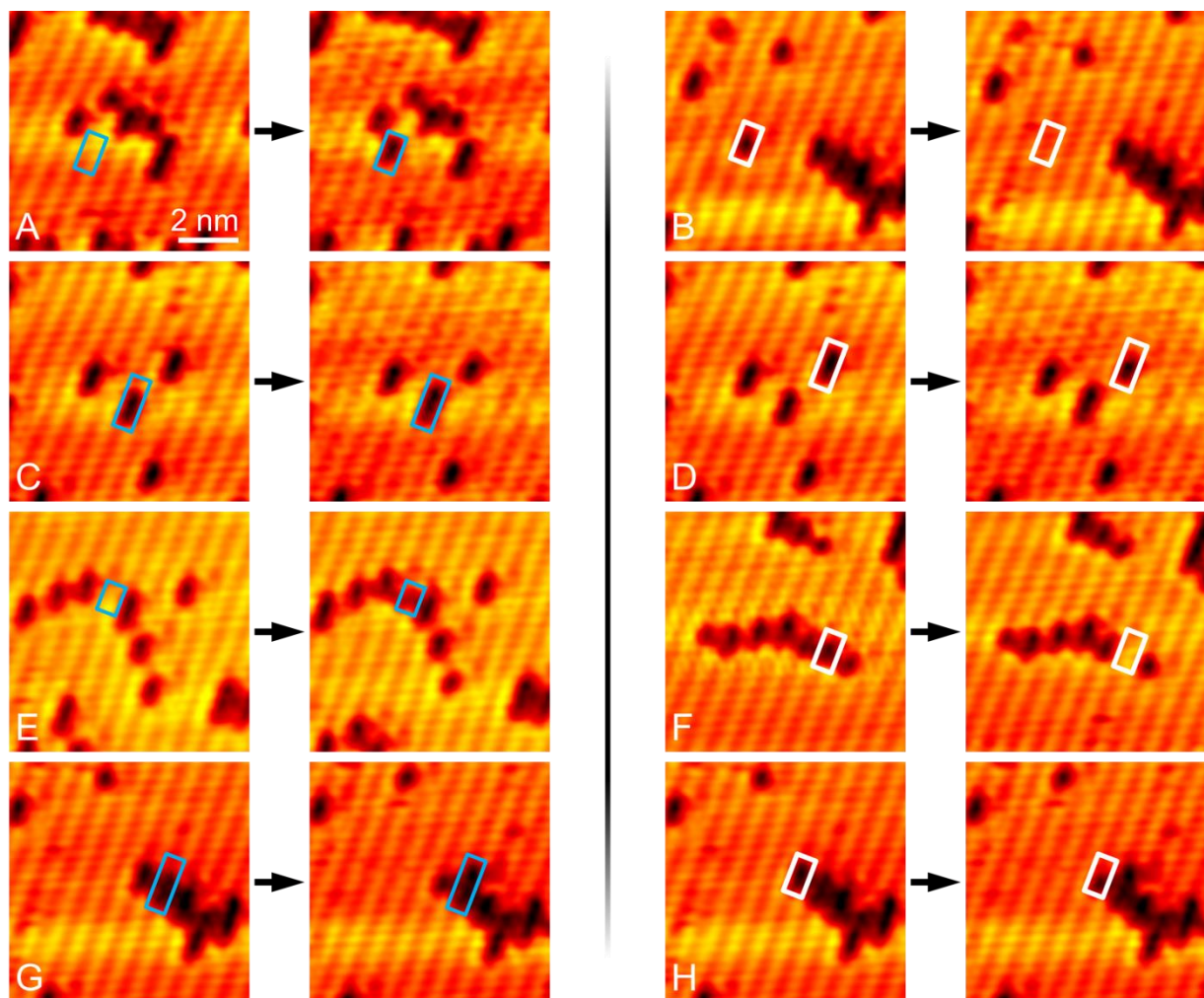


Figure S6. Corresponding STM images from Figure S5 but without superimposed atomic model.

Eight situations of oxygen migration were observed in STM in the presence of water at ~ 170 K (Fig. S5, S6). At the conditions, STM cannot capture the moving trajectories of oxygen movement. The oxygen migration is reflected as the addition or loss of oxygen atoms. When oxygen chain is short, made up by less than 3 oxygen atoms, the whole chain can be mobile regardless that if there is neighboring chains or not (Fig. S5A, S5B, S5E, S5F). Additionally, an existing oxygen chain can grow by accepting an oxygen atom in one end or shrink by losing an oxygen atom in one end (Fig. S5C, S5D, S5G, S5F). Again, the neighboring chain doesn't affect the mobility. Thus, oxygen-water interaction doesn't seem to be influenced by the inter-chain interaction. The corresponding original STM images are shown in Fig. S6.

2.3 O, H₂O and OH adsorption on Au(110)

Isolated O atoms on Au(110) are most stable in the pseudo 3-fold hollow site (Fig. S7 A) and have a binding energy of -3.71 eV relative to a gas phase O atom, in agreement with previous studies.² The binding strength of O on the Au(110) surface increases when O-atom chains are formed (binding energy -3.81 eV/per O for two-atom chain, -3.84 eV/per O for three-atom chain), in which O atoms are located at opposite sides of the Au atom ridge, forming a zig-zag configuration^{2, 7} (Fig. S7 B). Atomic

oxygen is an electrophilic adsorbate that withdraws electron density from the surface and behaves as a Brønsted base,⁸ inducing surface strain locally upon adsorption. Details about the bond lengths and charge exchange between the adsorbates and the surface are given in Table S2. Charge density difference plots (Fig. S7 A, B) illustrate the O-induced charge redistribution at the interface upon adsorption: a single O atom withdraws electron density from the 3 neighboring Au atoms (Table S2, S3), rendering them positively charged.²⁻⁹ The three Au atoms move away from each other to accommodate O atom adsorption, as discussed previously;² the charge exchange between the surface and O increases at higher oxygen coverage (Table S2, S3), which is expected since the adsorption energy per O is stronger by approximately 0.15 eV. Adsorption induced surface strain is observed with the Au-Au bond lengths decreasing at the ends of the zig-zag chain and extending locally in the middle of the chain to accommodate O adsorption (Table S3).

A single H₂O molecule on Au(110) binds weakly to the surface through the O atom at on-top position, at a distance 2.59 Å above it (Fig. S7 C) and with binding energy equal to -0.27 eV relative to a H₂O molecule in vacuum. There is no discernible change in surface structure due to the weak binding of H₂O on Au(110) is in agreement with experiment.¹⁰

Hydroxyl adsorption at sites a, b, c, d on Au(110) were investigated (Fig. S7D), with binding energies of -2.80 eV, -2.79 eV, -2.71 eV and -2.60 eV respectively. An isolated OH molecule bonds most stably at a 3-fold hollow site, although the bonding is not symmetric with bond distances 2.27, 2.22 and 2.42 Å with atoms Au₁, Au₂ and Au₃, (Table S2). Similar to an O atom, OH adsorption induces surface strain to the surface and charge depletion from the nearby Au atoms. (Table 1, Fig. S2 D). Compared to O adsorption, the charge exchange of OH with Au is smaller, consistent with the longer bond distances between OH and the Au atoms at the adsorption site.

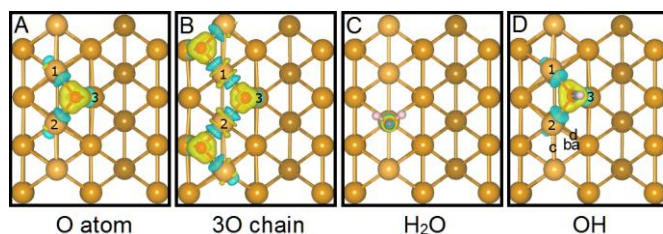


Figure S7. On top representation of the adsorption configurations and charge density difference isosurfaces for A) O atom, B) 3O atom chain, C) H₂O and D) OH on the Au(110) surface. Gold, red and white spheres represent gold, oxygen and hydrogen atoms respectively. Yellow (blue) contour depicts charge accumulation (depletion). Isosurface levels are at $\pm 0.004 e/\text{Bohr}^3$.

Structure	Distance from Au (Å)			Charge Transfer Δq (e)			
	d_{Au1}	d_{Au2}	d_{Au3}	d_{O-H} (Å)		$\Delta q_{(Au)}$	$\Delta q_{(O, H_2O, OH)}$
O	2.12	2.12	2.18	--		-0.80	+0.80
H ₂ O	--	2.59	--	0.98	0.98	+0.05	-0.05
OH	2.27	2.22	2.42	0.98		-0.49	+0.49

Table S2. Bond distances of oxygen, water and hydroxyl species on Au(110) and corresponding Bader charge transfer (Δq).

Structure		Distance from Neighboring Au (Å)			Charge Transfer Δq (e)	
					$\Delta q_{(Au)}$	$\Delta q_{(O)}$
2O chain	$d_{terminalO1-Au}$	2.01	2.12	2.19	-0.82	+0.82
	$d_{terminalO2-Au}$	2.01	2.12	2.19	-0.82	+0.82
3O chain	$d_{terminalO1-Au}$	2.01	2.11	2.17	-0.83	+0.83
	$d_{middleO-Au}$	2.01	2.01	2.17	-0.85	+0.85
	$d_{terminalO2-Au}$	2.01	2.11	2.17	-0.83	+0.83

Table S3. Bond distances of oxygen atoms in a 2-oxygen-atom and 3-oxygen-atom chain on Au(110) surface and corresponding Bader charge transfer (Δq).

2.4 Coadsorption of H₂O+O and OH+OH complexes on Au(110)

In this section we provide detailed information about the bond lengths of the coadsorbed configurations H₂O+O, OH+OH (a) and, OH+OH (b) that were discussed in the main article along with their corresponding charge density exchange with the Au(110) surface, calculated from Bader analysis.

The strong attractive interaction between H₂O and O in the coadsorbed complex H₂O+O increases the binding strength of H₂O on Au(110) and also induces surface strain locally upon adsorption. As a result, the O-H bonds in the H₂O molecule are strained, compared to an isolated H₂O molecule (Table S4). The calculated Bader charges quantify the charge density exchange between the adsorbates H₂O, O and the Au (110) surface and charge density difference plots show schematically the charge distribution between the surface and the adsorbed species (Table S4, Fig. S8 A). More specifically, in configuration H₂O+O one of the protons in the water is in close proximity (within 1.58 Å) to the adsorbed O, demonstrating that the strong attractive interaction and the stabilization of H₂O on the surface in the presence of a nearby O atom can be attributed at least in part to significant H bonding between H₂O and O. The O-H bonds are significantly modified, compared to an isolated H₂O molecule (1.03 and 0.97 Å). The O atom is located at a bridge site between Au atoms 1 and 2, and its bonds with the surface are now shorter compared to a single O atom (Table S4). The structural changes induced on the surface upon adsorption and the attractive interaction between H₂O and O also reflect in the charge density distribution between the adsorbates and the surface (Fig. S8 A, Table S4). The total charge depleted from the Au

surface is now partitioned between the two coadsorbed species with the O atom accumulating 0.62 electrons and the H₂O molecule 0.18 electrons, respectively.

In configuration OH+OH (a), the two OH molecules are in close proximity to each other (the proton of OH₁ is only 1.88 Å away from OH₂) and the attractive interaction between the two molecules arises from strong hydrogen bonding between them (Fig. S8 A). The amount of charge depleted from the Au surface is equally partitioned between the two OH molecules (Table S4). In configuration OH+OH (b), which is the resulting mirror image of A, the two OH molecules are 2.31 Å apart and experience an attractive interaction of 0.03 eV.

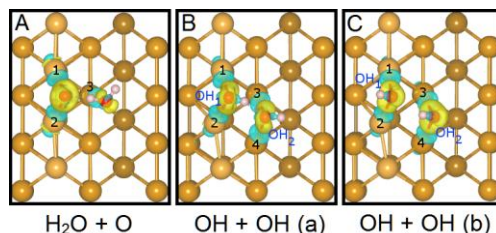


Figure S8. On top representation of the adsorption configurations and charge density difference isosurfaces for A) H₂O+O, B) OH+OH (a) and C) OH+OH (b) on the Au(110) surface. Gold, red and white spheres represent gold, oxygen and hydrogen atoms respectively. Yellow (blue) contour depicts charge accumulation (depletion). Isosurface levels are at ± 0.004 e/Bohr³.

Structures	Distance from Au (Å)				Charge Transfer Δq (e)	
	d_{Au1}	d_{Au2}	d_{Au3}	d_{O-H} (Å)	$\Delta q_{(Au)}$	$\Delta q_{(O,H_2O)}$
O + H ₂ O (b)						
O	2.07	2.07			-0.80	+0.62
H ₂ O	--	--	2.41	1.03,0.97		+0.18

Structures	Distance from Au (Å)					Charge Transfer Δq (e)	
	d_{Au1}	d_{Au2}	d_{Au3}	d_{Au4}	d_{O-H} (Å)	d_{OH-OH} (Å)	$\Delta q_{(OH)}$
OH+OH (a)							
OH ₁	2.19	2.16	--	--	0.99	1.88	0.50
OH ₂	--	--	2.26	2.34	0.98		0.41
OH+OH (b)							
OH ₁	2.25	2.18			0.98	2.31	0.41
OH ₂			2.22	2.26	0.98		0.18

Table S4. Bond distances of coadsorbed H₂O+O and OH+OH species on Au(110) and corresponding Bader charge transfer (Δq).

References

1. B. Xu, R. J. Madix and C. M. Friend, *J Am Chem Soc*, 2010, **132**, 16571-16580.
2. F. Hiebel, M. M. Montemore, E. Kaxiras and C. M. Friend, *Surf. Sci.*, 2016, **650**, 5-10.
3. P. A. Redhead, *Vacuum*, 1962, **12**, 203-211.
4. C. T. Campbell, L. Arnadottir and J. R. V. Sellers, *Zeitschrift Fur Physikalische Chemie-International Journal of Research in Physical Chemistry & Chemical Physics*, 2013, **227**, 1435-1454.

5. K. W. Kolasinski, *Surface science: foundations of catalysis and nanoscience*, John Wiley & Sons Ltd, Second edn., 2008.
6. J. L. Falconer and R. J. Madix, *J. Catal.*, 1977, **48**, 262-268.
7. M. Landmann, E. Rauls and W. G. Schmidt, *The Journal of Physical Chemistry C*, 2009, **113**, 5690-5699.
8. D. A. Outka and R. J. Madix, *Journal of the American Chemical Society*, 1987, **109**, 1708-1714.
9. D. Hibbitts and M. Neurock, *Surf. Sci.*, 2016, **650**, 210-220.
10. R. Liu, *Computational and Theoretical Chemistry*, 2013, **1019**, 141-145.